Food Chemistry: X 24 (2024) 101908

Contents lists available at ScienceDirect

Food Chemistry: X

journal homepage: www.sciencedirect.com/journal/food-chemistry-x

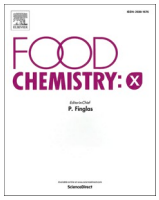

Structural characteristics and antioxidant activity of a low-molecular-weight jujube polysaccharide by ultrasound assisted metal-free Fenton reaction

Yingying Liu [a,b,c,1], Yan Meng [d,1], Haozhen Ji [a,b], Jianhang Guo [a,b], Miaomiao Shi [a,b], Feiliao Lai [e,**], Xiaolong Ji [a,b,c,*]

[a] College of Food and Bioengineering, Zhengzhou University of Light Industry, Zhengzhou 450001, China
[b] National & Local Joint Engineering Research Center of Cereal-Based Foods (Henan), Zhengzhou 450001, China
[c] Key Laboratory of Cold Chain Food Processing and Safety Control, Ministry of Education, Zhengzhou University of Light Industry, Zhengzhou 450001, China
[d] School of Pharmacy, Hubei University of Chinese Medicine, Wuhan 430065, China
[e] Department of Physics, School of Science, Tianjin University, Tianjin 300072, China

ARTICLE INFO

Keywords:
Ultrasound assisted H_2O_2/V_C reaction
Jujube polysaccharide
Structure
Antioxidant activity

ABSTRACT

This study used an ultrasonically accelerated metal-free Fenton (H_2O_2-V_c system) reaction to promote water-extracted degrading polysaccharides from *Ziziphus Jujuba cv. Muzao* (DZMP). A novel jujube polysaccharide (DPZMP3) was obtained by degradation using DEAE-Sepharose Fast Flow and Sephacryl S-100 column chromatography. Methylation analysis, HPGPC, ion chromatography, FT-IR, and NMR spectroscopies were used to clarify the chemical structures of DPZMP3. Monosaccharide compositional analysis of DPZMP3 revealed the presence of Rha, Ara, Gal, and GalA at a molar ratio of 1.00:1.49:1.60:7.68, and the HPGPC data demonstrated the average *Mw* of 34.3 kDa. Based on the structural and linkage research using NMR spectroscopy and GC–MS, it was determined that DPZMP3 was a homogalacturonan pectic polysaccharide with a (1 → 4)-Gal*p* branch at C-6 and a small amount of Ara*f* and Rha*p* residues. The ultrasonic-aided Fenton treatment did not significantly alter the structure of DPZMP3. It may also be useful for DZMP and enhancing their antioxidant activity *in vitro*. The current study's findings could pave the way for the food sector to use jujube polysaccharides obtained by degradation as a functional food component.

1. Introduction

One of the world's oldest fruit trees that have been grown, the jujube is the ripe fruit of the genus *Ziziphus*. It is mainly distributed in Xinjiang, Hebei, Shandong, Shaanxi, Henan, Ningxia, Shanxi, and other places in China. Scholars have conducted in-depth research on the pharmacological activities of jujube, and the findings show that jujube has a variety of pharmacological actions, including immunological control, anti-inflammatory, anticancer, antihyperglycemic, antioxidant, and gut microbiota regulation (Gao et al., 2013). Chemical research has shown a direct relationship between the pharmacology of jujube and its abundance of bioactive components, including dietary fiber, amino acids, polysaccharides, polyphenols, flavonoids, nucleotides, and others (Aafi et al., 2022). Among them, one of the key bioactive ingredients in jujube fruit is polysaccharides, which have a range of bioactivities. Structural studies have shown that the structure of jujube polysaccharides is closely related to their pharmacological activity and that structural modification also could enhance the pharmacological activity (Li et al., 2022). Prior research has shown that the primary polysaccharide in jujube was rhamnogalacturonan II (RG II) (Yang et al., 2021), rhamnogalacturonan I (RG I) (Wang et al., 2015), and homogalacturonan (HG) (Zhan et al., 2018), *etc.*

Chain conformation, functional group, molecular weight (*Mw*), glycosidic linkage, monosaccharide content, degree of branching, and other structural characteristics are all strongly connected to the functional characteristics of plant polysaccharides, a class of complex

* Corresponding author at: College of Food and Bioengineering, Zhengzhou University of Light Industry, China.
** Corresponding author at: Department of Physics, School of Science, Tianjin University, China.
E-mail addresses: laifeiliao@gmail.com (F. Lai), xiaolongjiytu@163.com (X. Ji).
[1] These authors contributed equally to this work.

https://doi.org/10.1016/j.fochx.2024.101908
Received 11 August 2024; Received in revised form 12 October 2024; Accepted 16 October 2024
Available online 20 October 2024

biomacromolecules (Wu, He, et al., 2022). Numerous research has shown that polysaccharides with a lower *Mw* were more likely to have better antioxidant activity (Lee et al., 2023; Liu et al., 2010). Degradation of polysaccharides has been shown to enhance their antioxidant properties, which may be attributed to the fact that after the treatment, the molecular chain of polysaccharide is broken, and more active groups are exposed to the solution, which makes it easier to create contact between active sites and free radicals (Chen et al., 2020). *Grateloupia livida*'s sulphated polysaccharides were broken down by Chen et al. (2020) using microwave therapy and Vc-H_2O_2. *In vitro* tests were conducted to boost the broken-down polysaccharides' antioxidant potential. After applying H_2O_2-Vc-ultrasonic and H_2O_2-Fe^{2+}-ultrasonic treatments to *Codium cylindricum*, Yan et al. (2021) was able to extract two polysaccharides obtained by degradation with lower *Mw*s than typical polysaccharides were shown to have higher antioxidant qualities based on the findings of their *in vitro* antioxidant activity. The plant polysaccharides contain the higher uronic acid levels and exhibit stronger *in vitro* antioxidant activity. The close relations are between arabinose (1 → 4) and mannose (1 → 2) to reducing power, and glucose (1 → 6) and arabinose (1 → 4) to DDPH radical scavenging (Lo et al., 2011).

The jujube polysaccharides have various biological activities, but their entry into the cell for biological activity is limited owing to their larger *Mw*, higher polymerization, and poorer water solubility. Degrading jujube polysaccharides hence requires the development of effective, time-saving, environmentally benign, and non-destructive technologies (Ji et al., 2023; Wang et al., 2023). In recent years, there are several ways to degrade polysaccharides, such as combination degrading methods, and physical, chemical, and biological procedures (Hu et al., 2023). Physical procedures, such as microwave, high-pressure micro fluidization, irradiation, pulsed electric field, ultrasound, and plasma, are effective and environmentally benign, but they also need more equipment and produce comparatively less degradation products (Wu, Zhao, et al., 2022). Chemical degradation is very convenient to operate, such as the hydrolysis of acid or alkaline substances and the breakdown of hydrogen peroxide. However, chemical degradation is not friendly to the environment and the different reactions difficult to control. Biological methods mainly including enzymatic hydrolysis and microbial fermentation, is a mild, green, and high degradation efficiency way to degrade polysaccharide, nonetheless, due to the intricate architectures of polysaccharides, screening of enzymes and microorganisms is necessary (Wang et al., 2021). Since every technique has its own drawbacks, it is imperative to create new technologies in order to get reduced *Mw* polysaccharides. The maximum amount of antioxidant activity was discovered by Li et al. (2020) in the *Tremella fuciformis* polysaccharides that were broken down using the ultrasonic-assisted H_2O_2-V_C technique. The combination of several degradation techniques has garnered significant interest owing to its better effectiveness and ability to compensate for the inadequacies of a single degradation approach. One such method is the H_2O_2-Vc coupled with ultrasonic treatment (Wu, He, et al., 2022). Therefore, H_2O_2-Vc-ultrasonic might be used to break down the jujube polysaccharides; however, there is no record of this technique being applied to break down jujube polysaccharides in order to enhance their bioactivities.

As a result, the DPZMP3 was generated by ultrasonic aided H_2O_2/Vc treatment, and it was purified using DEAE-Sepharose Fast Flow and Sephacryl S-100 in order to demonstrate the impact of this treatment on the jujube polysaccharides' structural and biological functions. Next, the *in vitro* antioxidant activity and structural properties of DPZMP3 were examined.

2. Materials and methods

2.1. Reagents

GE Healthcare Life Sciences (Piscataway, NJ, USA) provided the exchange of anion Sephacryl S-100 and DEAE-Sepharose Fast Flow. Loess Plateau Experimental Orchard provided the jujube fruit (*Ziziphus Jujuba cv. Muzao*). The grade of all other compounds was analytical.

2.2. Degradation polysaccharides from Z. jujuba cv. Muzao preparation

The crude *Z. jujuba cv. Muzao* polysaccharides (ZMP) were extracted in accordance with other reports (Ji, Peng, Li, et al., 2017). A 40 kHz fixed frequency ultrasonic processor with a 480 W maximum power was used to carry out the ultrasound-H_2O_2/Vc degradation of ZMP in accordance with the adjustments made to earlier research (Li et al., 2020; Wu, Zhao, et al., 2022). The conditions of ultrasound-H_2O_2/Vc reaction were as follows: Vc/H_2O_2 concentration 10.0 mM, temperature 51 °C, time 65 min; under these optimal conditions, in terms of radical scavenging efficiency, 1,1-diphenyl-2-picrylhydrazyl (DPPH) yielded 72.16 % and 81.76 % of degradation *Z. jujuba cv. Muzao* polysaccharide (DZMP) (Guo et al., 2024). According to the chemical analysis, DZMP had a protein content of 1.14 % and a carbohydrate content of 81.78 %, respectively, whereas ZMP had a protein content of 2.35 % and 75.47 %.

2.3. Purification of DPZMP3

The DZMP (300 mg) was diluted in deionized water (10 mL) and then put on a DEAE-Sepharose Fast Flow column. It was then eluted with deionized water and NaCl solutions (0.1, 0.2, and 0.3 M), respectively. After that, it underwent enrichment, concentration, dialysis, and lyophilization. The results were labeled DZMP1, DZMP2, DZMP3, and DZMP4. To further boost the purity of the four fractional polysaccharides, a Sephacryl S-100 gel column was employed for purification. Collecting the corresponding sugar peaks, enrichment, concentration, lyophilization, and yielded purified polysaccharides, which were named DPZMP1, DPZMP2, DPZMP3, and DPZMP4. The largest fraction (DPZMP3) was to be obtained for further study.

2.4. Physical and chemical property analysis

2.4.1. Analysis of chemical components

The purified jujube polysaccharides obtained by degradation (DPZMP1, DPZMP2, DPZMP3, and DPZMP4) may have their total sugar content measured thanks to the use of the phenol-sulfuric acid procedure. We used the Coomassie brilliant blue technique to evaluate the protein content. With the Folin-Ciocalteu colorimetric technique, the total phenol concentration was ascertained (Ji et al., 2021).

2.4.2. Molecular weight

Using a RI-10 A detector fitted with a BRT105–104-102 tandem gel column (8 × 300 mm), high-performance liquid gel chromatography (HPGPC) was chosen to evaluate the *Mw* of DPZMP3. The following were the parameters of the experiment: injection volume (20 μL), column temperature (40 °C), flow rate (0.6 mL/min), mobile phase (0.05 M NaCl solution), and DPZMP3 concentration (5 mg/mL).

2.4.3. Analysis of monosaccharide composition

The ion chromatography was used to assess the monosaccharide content of DPZMP3. After weighing and completely dissolving 5 mg of DPZMP3 in 2 mL TFA (3 M), the mixture was hydrolyzed for three hours at 120 °C in an oven. Following the hydrolysis process, the mixture was mixed with 5 mL of deionized water, then ethanol was added to eliminate the TFA. Aspirate 50 μL of the mixture, add 950 μL deionized water, centrifuge, and pass the mixture through an ion chromatography analysis-ready 0.22 μm filter membrane. The parameters were as follows: injection volume (5 μL), flow rate (0.3 mL/min), mobile phases (A: H_2O, B: 15 mM NaOH, C: 100 mmol/L NaOAC), column temperature (30 °C), and Dionex Carbopac TM PA20 (3 × 150 mm) (Ji et al., 2019).

2.4.4. Fourier transform-transformed infrared (FT-IR) and ultraviolet

UV spectrum scanning was carried out in the 200–400 nm range using the specified 0.5 mg/mL DPZMP3 solution. The infrared spectrum was scanned in the 400–4000 cm^{-1} frequency band after 300 mg of KBr and 3 mg of dry DPZMP3 (which had been baked at 105 °C for 4–6 h) were combined, ground, and formed into tablets (Ji, Yan, et al., 2020).

2.4.5. Methylation examination

With a few adjustments, the methylation study of DPZMP3 was carried out in accordance with previously published procedures. The DPZMP3 was first carboxyl-reduced by EDC and $NaBD_4$. 2–3 g of DPZMP3 were weighed into a reaction container. 1 mL of DMSO and anhydrous alkali solution were then added to thoroughly dissolve the material. Next, methyl iodide solution was added, and finally, 2 mL of ultrapure water were added to conclude the reaction. Added 1 mL TFA (2 M) to the lyophilized recovered methylated DPZMP3 sealed hydrolysis for 90 min. After reacting the hydrolysate for 8 h at room temperature with double-distilled water (2 mL) and sodium borohydride (60 mg), the reaction was neutralized by lowering the glacial acetic acid. Then 1 mL acetic anhydride was added and the reaction was carried out at 100 °C for 1 h for acetylation, the reaction was allowed to cool to room temperature in order to remove any excess acetic anhydride. Ultimately, the organic layer was collected and the acetylation production was extracted using CH_2Cl_2. The organic layer was then passed through a filter membrane (0.45 μm), with the volume set at 10 mL. The following were the chromatographic conditions for the GC–MS: Using a column (30 m × 0.25 mm × 0.25 μm) and an RXI-5 SIL MS detector, the temperature was raised by 3 °C every minute, from 120 °C to 250 °C. The temperature was then held for five minutes.

2.4.6. Nuclear magnetic resonance (NMR) spectrum

A Bruker NMR spectrometer (AVIII-600) was used to weigh and dissolve 50 mg of DPZMP3 in D_2O. Two-dimensional (HSQC, HMBC, TOCSY, and COSY spectra) and one-dimensional (^1H and ^{13}C NMR spectra) spectra were also acquired at 303 K.

2.5. Antioxidant activities analysis

2.5.1. Scavenging activity of DPPH

With a few modest adjustments, the DPPH radical scavenging rate was determined using a prior technique (Ji, Hou, et al., 2020). After mixing DPZMP3 solution (2 mL, 1 mg/mL) at various concentrations with DPPH-ethanol solution (2 mL, 0.1 mM), the mixture was allowed to react without exposure to light (37 °C, 30 min). Then, we measured the absorbance at 517 nm. The following formula was used to compute the DPPH radical scavenging rate, with Vc acting as a positive control:

$$\text{DPPH scavenging activity } (\%) = \left(1 - \frac{A_1 - A_2}{A_0}\right) \times 100$$

in this case, A_1 stood for the sample group absorbance, A_2 for the blank group absorbance, and A_0 for the control group absorbance.

2.5.2. Activity of superoxide radical scavenging

With a few minor adjustments, the prior procedure was used to calculate the superoxide radical scavenging capability (Yan et al., 2021). The reaction was conducted in a water bath (25 °C, 20 min) after adding and thoroughly mixing Tris-HCl solution (2 mL, 50 mM, pH 8.2). 0.4 mL of DPZMP3 was also added. Next, 2 mL of pyrogallol (7 mM) were added and well combined. Addition of HCl (0.4 mL, 10 mM) terminated the reaction after 5 min of operation at 25 °C. Using Vc as the positive control, the solution's absorbance at 420 nm was determined. The superoxide radical's ability to be scavenged was calculated using the following formula:

$$\text{Superoxide radical scavenging activity } (\%) = \left(1 - \frac{A_1 - A_2}{A_0}\right) \times 100$$

where the sample groups' absorbances (A_1), the blank group's absorbance (A_2), and the control group's absorbance (A_0).

2.5.3. Activity of hydroxyl radical scavenging

The prior procedure was chosen to ascertain the rate of hydroxyl radical scavenging (Ji, Hou, et al., 2020). 1 mL of DPZMP3 solution at various concentrations was combined with $FeSO_4$ (1 mL, 6 mM), salicylic acid-ethanol solution (1 mL, 6 mM), and H_2O_2 (1 mL, 6 mM) solution. The mixture was then agitated and allowed to react (30 min, 37 °C). Based on the absorbance of the solution measured at 517 nm, the following equation was used to compute the hydroxyl radical scavenging rate:

$$\text{Hydroxyl radical scavenging } (\%) = \left(1 - \frac{A_1 - A_2}{A_0}\right) \times 100$$

in this case, A_1 stood for the sample group absorbance, A_2 for the blank group absorbance, and A_0 for the control group absorbance.

2.6. Analytical statistics

SPSS and Origin 2018 were used to plot and statistically analyze the experimental data. The mean ± standard deviation was used to depict the experimental results.

3. Result and discussion

3.1. Separation and purification

Using ultrasound-assisted H_2O_2/Vc reaction, DZMP with a yield of 72.16 % were obtained from *Z. jujuba cv. Muzao* polysaccharides (ZMP) (Guo et al., 2024). Then, using water and NaCl (0.1, 0.2, and 0.3 M), the purified jujube polysaccharides obtained by degradation (DZMP1, DZMP2, DZMP3, and DZMP4) were eluted using the DEAE-Sepharose Fast Flow chromatographic column (Fig. 1A). An S-100 gel column from Sephacryl was then used to purify each fraction, and the matching sugar peaks-which were subsequently termed DPZMP1, DPZMP2, DPZMP3, and DPZMP4 were enriched, concentrated, and lyophilized (Fig. 1B-E).

3.2. Chemical components analysis

Four jujube polysaccharides obtained by degradation, including DPZMP1, DPZMP2, DPZMP3 and DPZMP4 (DZMPs), were prepared effectively, and the corresponding yields were 16.33 %, 0.68 %, 5.37 %, and 0.94 %, respectively, based on DZMP. Table 1 showed the chemical components of DZMPs, including carbohydrate, protein, and total phenol. The carbohydrate and proteins contents varied from 89.41 % to 95.81 % and 0.52 % to 1.05 %, respectively, in DZMPs. For study and analysis, DPZMP3, which had a lower protein content and a greater total sugar content, was used. In comparison to PZMP2 (96.92 %, eluted with DEAE-Sepharose Fast Flow and 0.2 M NaCl and Sephacryl S-300 columns) (Ji et al., 2019) and PZMP3 (96.56 %, eluted with 0.3 M NaCl) (Ji, Yan, et al., 2020), there were no notable alterations in the carbohydrate content of DPZMP3. Though not clearly affecting the total sugar content of jujube polysaccharides, the small variations in carbohydrate content may be explained by the action of ·OH produced by the H_2O_2-Vc system, which might break the primary sugar chain (Wu, Zhao, et al., 2022).

3.3. Mw and monosaccharide compositions

Plant polysaccharides' expected uses and bioactivities are often greatly influenced by their *Mw* (Wu, He, et al., 2022). The $R^2 = 0.9943$

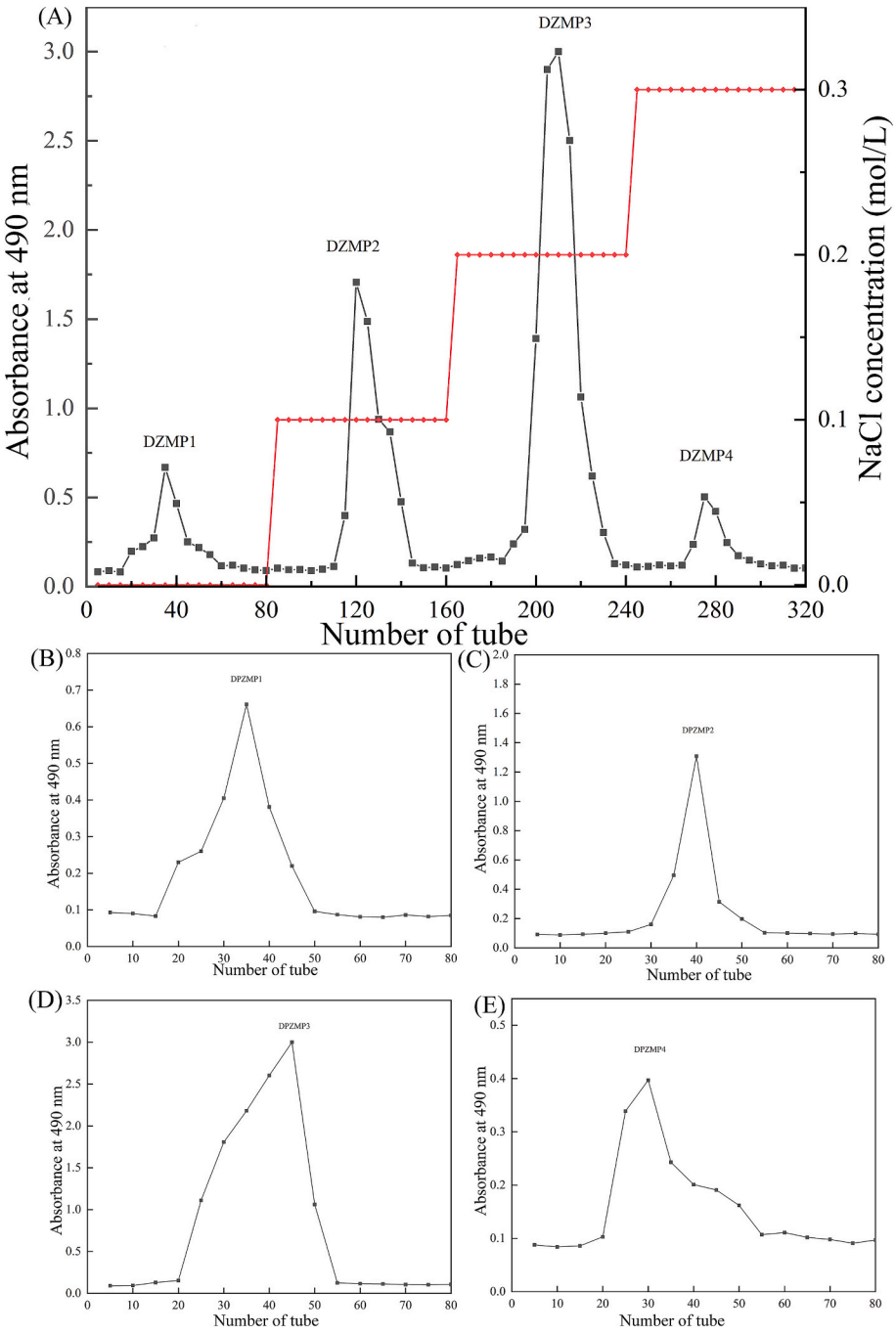

Fig. 1. The flow diagram for separation of DPZMPs.

Table 1
Chemical composition of DPZMPs.

Samples	Yield (DZMP amount)(%)	Total carbohydrate content(%)	Protein content (%)	Total phenol content (mg GAE/100 g)
DPZMP1	0.94	89.41 ± 1.35^{b}	1.05 ± 0.13^{a}	0.25 ± 0.03^{b}
DPZMP2	5.37	94.26 ± 0.72^{a}	0.69 ± 0.08^{c}	0.13 ± 0.05^{c}
DPZMP3	16.33	95.81 ± 1.20^{a}	0.52 ± 0.05^{d}	0.21 ± 0.04^{c}
DPZMP4	0.68	90.84 ± 0.96^{b}	0.83 ± 0.07^{b}	0.37 ± 0.06^{a}

Different letters in the same column indicate a significant difference at $P<0.05$.

and y = −0.1924× + 12.2 was the equation of the lg*Mw*-RT curve developed based on the dextran specimens with varied *Mw*s. DPZMP3's related BRT105–104-102 chromatogram, as shown in Fig. S1A, included a single symmetrical peak, suggesting that the polysaccharide component was homogenous. PZMP2 had a *Mw* of 62.73 kDa, whereas PZMP3 had a *Mw* of 58.21 kDa, in the prior report were higher than the average *Mw* of 34.3 kDa, as shown by the retention time (39.84 min) (Ji et al., 2019; Ji, Yan, et al., 2020). This result suggested that DPZMP3 was obviously obtained by ultrasound assisted H_2O_2-Vc reaction, and the *Mw* decreased obviously with reaction time (Wu, Zhao, et al., 2022). The shear forces and reactive free radicals generated by the ultrasound/H_2O_2 system could be the main factors affecting the *Mw* of degradation jujube polysaccharides. This result was consistent with that *Passiflora edulis* peel polysaccharide (Li et al., 2021), *Codium* cylindricum polysaccharide

(Yan et al., 2021), and okra pectic-polysaccharides (Wu, He, et al., 2022).

Plant polysaccharides' natural basic unit, monosaccharide compositions, has been shown to have a considerable influence on the structures and functional properties of polysaccharides that are found in natural plant sources (Yuan et al., 2020). DPZMP3 was shown to be a heteropolysaccharide higher in galacturonic acid according to the monosaccharide composition analysis. It was found to include Rha, Ara, Gal, and GalA, with molar ratios of 1.00:1.49:1.60:7.68 (Fig. S1C). The kinds of monosaccharide compositions of DPZMP3 were not significantly different from those of PZMP2 (GalA, Gal, Xyl, Ara, Rha/2.20: 2.68: 0.22: 5.23: 1.18, type RG-I) (Ji et al., 2019) and PZMP3 (GalA, Gal, Ara, Rha/18.69: 1.00: 2.00: 1.74, type HG-like pectin) (Ji, Yan, et al., 2020). According to the findings, which were consistent with earlier research (Wu, Zhao, et al., 2022; Yeung et al., 2021), the ·OH produced by the H_2O_2-Vc system may target the side chains and the backbone of RG-I (1,2,4-Rha*p*). In summary, the results demonstrated that DPZMP3's molar ratios were impacted by the ultrasound-assisted H_2O_2/Vc treatment, while the kind of primary structure and monosaccharide compositions remained unchanged (Yuan et al., 2020).

3.4. Analysis of UV and FT-IR spectra

In accordance with the findings of the chemical test, DPZMP3 did not include proteins or nucleic acids, as shown by the lack of absorption at 260 and 280 nm in Fig. 2A (Wang et al., 2021). Therefore, the purity of DPZMP3 was relatively higher. Plant polysaccharide functional groups are often analyzed qualitatively using the FT-IR method. With FT-IR spectroscopy, the main functional groups of DPZMP3 were examined in the 4000–500 cm^{-1} range. The -OH stretching vibrations of DPZMP3 exhibited a broad and robust peak at 3413 cm^{-1}, whereas the C—H bending vibration absorption peak was located at 2933 cm^{-1}, as seen in Fig. 2B (Ma et al., 2014). However, the absorption bands that were seen at 1612 cm^{-1} and 1419 cm^{-1}, respectively, were caused by the asymmetric stretching of the COO- and C—H (O—H) vibrations that caused the C═O bond (Wu, He, et al., 2022). Moreover, C-O-C and C-OH stretching vibrations were detected in the absorption peaks at around 1200–1000 cm^{-1}, showing that the pyranose ring was present, DPZMP3 was identified as being of the β-type pyranose by an absorption peak at 894 cm^{-1} (Hajji et al., 2019). Interestingly, compared with PZMP2 and PZMP3 (Ji, Yan, et al., 2020), the intensity of absorption band associated with C═O asymmetric stretching (around 1601 cm^{-1} and 1420 cm^{-1}) in DPZMP3 gradually increased with the H_2O_2-Vc treatment. Consequently, the non-Gal*p*A residues in DPZMP3 were reactive with hydroxyl radicals during the ultrasound-assisted H_2O_2-Vc treatment, which led to the formation of fragments that were enriched in uronic acid (Gal*p*A) (Wu, Zhao, et al., 2022). Additionally, by disrupting the intermolecular and non-covalent intrabonds in plant pectic polysaccharide clusters, the ultrasound shear force process may contribute to the disintegration of these clusters during the initial stages of the ultrasound-assisted H_2O_2-Vc degradation reaction (Yan et al., 2021), thereby accelerating the degradation of DPZMP3.

3.5. Methylation examination

The glycosidic bond residues were further clarified by methylating, reducing, and acetylating DPZMP3, which was then subjected to GC–MS analysis. Based on their primary mass components in DPZMP3, the six linkage patterns were found (Table 2). 1,3,4-Gal*p*, T-Ara*f*, 1,4-Gal*p*/1,4-Gal*p*A, 1,5-Ara*f*, 1,2,4-Rha*p*, and 1,4,6-Gal*p* made up the majority of DPZMP3. Our calculations yielded the following molar ratios for the six sugar residues: 3.10:2.47:5.45:77.60:3.95, based on the peak area of the respective peaks. This result indicated that DPZMP3 contained 88.90 % Gal*p*A/Gal*p* residues, 5.45 % Rha*p* residues, and 5.57 % Ara*f* residues; according to the monosaccharide composition identified *via* GC, the primary structural component of DPZMP3 was 1,4-linked Gal*p*A (Ji et al., 2023). Besides, compared with the methylation analysis of PZMP2 (Rha*p*: Ara*f*: Gal*p*: Gal*p*A/11.86:39.44:30.54:18.16) (Ji et al., 2019) and PZMP3 (2.51:6.25:2.75:88.49) (Ji, Yan, et al., 2020), there was no apparently changes in DPZMP3, which could be explained by that the ultrasound assisted H_2O_2-Vc treatment did not change the repeating unit of DPZMP3.

Table 2
The results of methylation analysis for DPZMP3.

Peak No.	Residues	Retention time (min)	Methylated sugars	Linkage patterns	Relative amount (%)
1		16.121	2,3,5-Me_3-Ara*f*	T-Ara*f*	3.10
2		21.362	2,3-Me_2-Ara*f*	1,5-Ara*f*	2.47
3		23.563	3-Me-Rha*p*	1,2,4-Rha*p*	5.45
4	B/A	29.236	2,3,6-Me_3-Gal*p* 2,3,6-Me_3-Gal*p*A	1,4-Gal*p*/ 1,4-Gal*p*A	77.60
5		33.184	2,6-Me_2_Gal*p*	1,3,4-Gal*p*	3.95
6	C	36.116	2,3-Me_2-Gal*p*	1,4,6-Gal*p*	7.43

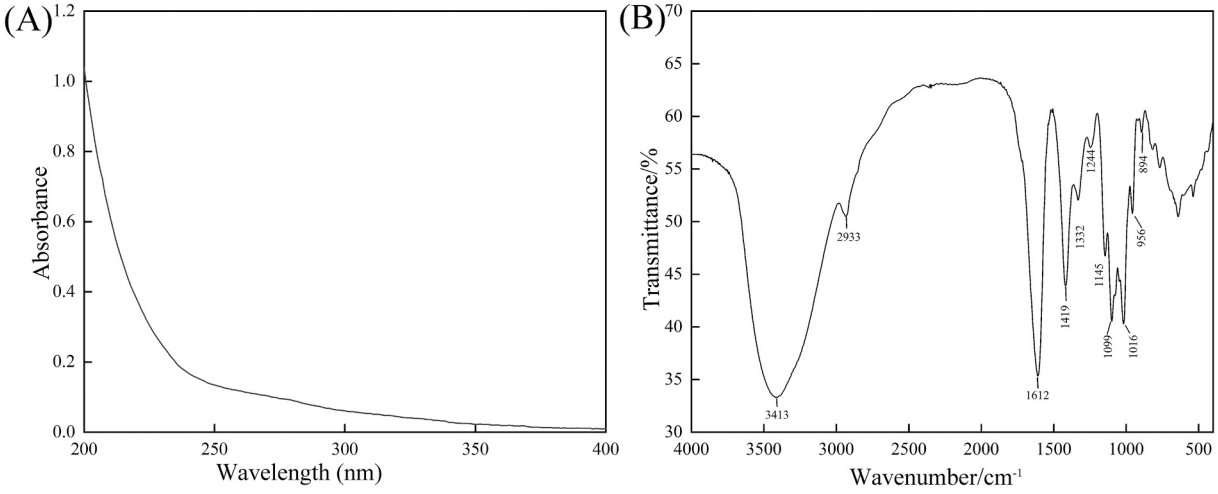

Fig. 2. The DPZMP3 physicochemical analysis. (A) UV–Vis spectrum. (B) FT-IR spectrum.

3.6. NMR analysis

The DPZMP3 structure was clarified by the use of the 1D (^{1}H, ^{13}C) and 2D (HSQC, COSY, TOCSY, and HMBC) NMR spectra (Fig. 3). Three primary anomeric proton signals (designated A, B, and C, respectively) at 5.16, 4.54, and 4.54 ppm were detected in the ^{1}H NMR spectra (Fig. 3A) of DPZMP3. The α-type was identified by signals beyond 5 ppm, while the *β*-type was identified by signals below 5 ppm (Li et al., 2011). The ^{1}H NMR spectra showed chemical shifts caused by protons in the residues from C-2 to C-6, which occurred from 4.70 to 3.62 ppm. Based on the small variations between their spectra from HSQC (Fig. 3C) and TOCSY (Fig. 3E), the chemical shifts of the corresponding carbon atoms had been inferred (Ji, Yan, et al., 2020). The ^{13}C NMR spectra (Fig. 3B) indicated the presence of uronic acid in DPZMP3, with three anomeric carbon signals in the 60–100 ppm range and one signal in the 170–180 ppm range. Table 3 was a compilation of the relevant NMR data for the three glycosidic linkages (Ji, Hou, et al., 2020). Using data from the HSQC, COSY, TOCSY, and HMBC (Fig. 3F) spectra, the ^{1}H and ^{13}C NMR assignments of all the tagged residues were made.

Three anomeric signals were detected in the ^{13}C NMR spectra at 99.1, 103.2, and 103.2 ppm. Using 2D NMR analysis and values from existing literature, as accurately as possible, all of the ^{1}H and ^{13}C signals were allocated (Ji, Hou, et al., 2020). For the cross-peak in the anomeric area of the HSQC spectrum at 175.5 ppm, a tentative attribution of Gal*p*A (residue A) was determined (Fig. 3C). According to prior findings (Ji, Yan, et al., 2020; Zhang et al., 2018), from the COSY and TOCSY spectra, calculated at 5.16, 3.70, 4.04, 4.34, and 4.70 ppm, respectively, were the chemical shifts of H-1, H-2, H-3, H-4, and H-5 (Fig. 3A). Based on the chemical shifts of the protons in the HSQC spectrum, the carbon chemical shift of residue A was identified as going from C-1 to C-5 (Table 3). This residue (A) had the same 1,4-linked Gal*p*A chemical shifts, according to the NMR data.

The methylation study findings and data from published literature showed that the B/C residues exhibited an anomeric signal at 4.54 ppm, which suggested that the B/C residue was galactose (Ji, Hou, et al., 2020). For H-1, H-2, H-3, H-4, H-5, and H-6, the proton chemical shifts of residue B were 4.54, 3.68, 3.94, 4.20, 3.73, and 3.80 ppm, respectively, based on the COSY (Fig. 3D) and TOCSY (Fig. 3E) spectra. Based on the proton chemical shifts of residue B (Table 3), the ^{13}C chemical shifts in the HSQC spectrum (Fig. 3C) for C-1, C-2, C-3, C-4, C-5, and C-6 were at 103.2, 69.4, 72.2, 68.7, 75.7, and 60.0 ppm, respectively. The carbon chemical shifts of residue B from C-1 to C-6 were almost in line with the usual values for a 1,4-linked Gal*p* methyl glycoside (Fei et al., 2024; Ji, Yan, et al., 2020). For 1,4,6-linked Gal*p*, the findings of methylation analysis and NMR tests suggest that the Gal*p* may produce one anomeric carbon/hydrogen signal at 69.0/3.85 ppm (Chen et al., 2019; Zhang et al., 2018), which may be designated as A and B.

Table 3
Assignments of ^{1}H and ^{13}C NMR spectra for DPZMP3.

Residues	Linkage		1	2	3	4	5	6
A	1,4-Gal*p*A	C	99.1	67.8	68.0	77.9	70.6	175.5
		H	5.16	3.70	4.04	4.34	4.70	
B	1,4-Gal*p*	C	103.2	69.4	72.2	68.7	75.7	60.0
		H	4.54	3.68	3.94	4.20	3.73	3.81
C	1,4,6-Gal*p*	C	103.2	69.3	71.9	68.7	76.1	69.0
		H	4.54	3.62	3.94	4.20	3.73	3.85

Determine the glycosidic connections of plant polysaccharides between sugar residues using the strong COSY (Fig. 3D) and HMBC (Fig. 3F) techniques (Ji, Yan, et al., 2020). Therefore, using these methods, Table 3 listed the intra-residue linkages of DPZMP3. The inter-residual cross-peaks listed below were also seen in the COSY spectrum: A/B/C H-1 to A/B/C H-2, A/B/C H-2 to A/B/C H-3, A/B/C H-3 to A/B/C H-4, A/B/C H-4 to A/B/C H-5, and B/C H-5 to B/C H-6, respectively. There were several inter-residual cross-peaks in the HMBC spectrum, ranging from A/B/C H-4 to A/B/C C-1.

We were able to conclude that the main component of DPZMP3's backbone was 1,4-Gal*p*A residues (HG-pectic polysaccharide), with (1 → 4)-Gal*p* branched at C-6 with some side chains Ara*f* and Rha*p* residues. These conclusions were based on the monosaccharide composition, FT-IR spectroscopy, HPGPC, GC–MS, as well as 1D and 2D NMR spectroscopy analyses of DPZMP3. These outcomes also demonstrated that the main structure of DPZMP3 was not altered by the ultrasound-assisted H_2O_2-Vc therapy.

3.7. Antioxidant properties of DPZMP3 in vitro

Comparing the three jujube polysaccharide fractions (DPZMP3,

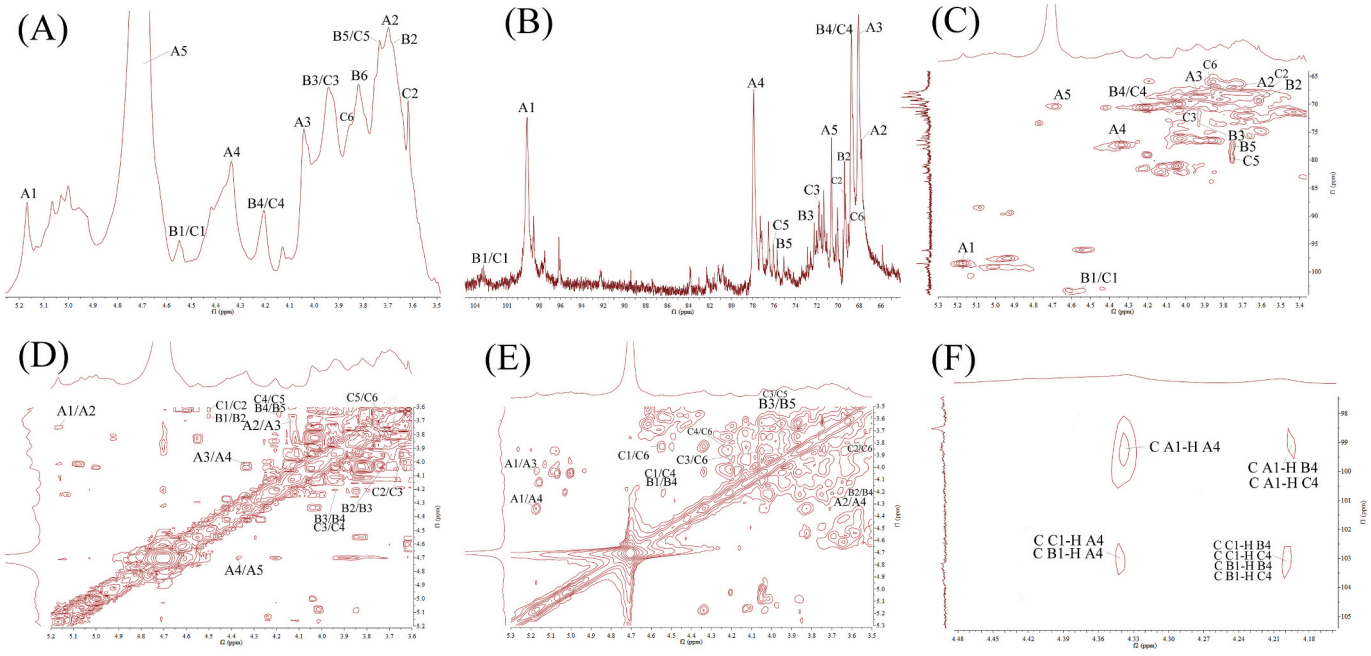

Fig. 3. The DPZMP3 in D_2O NMR spectra. (A) ^{1}H spectra. (B) ^{13}C spectra. (C) HSQC spectra. (D) COSY spectra. (E) ^{1}H/^{1}H TOCSY spectra. (F) HMBC spectra.

DZMP, and ZMP) to V_C, the radical (DPPH, $\cdot O^{2-}$, and ·OH) scavenging capabilities were assessed (Fig. 4). Because of its ease of use and repeatability, to determine how well various plant polysaccharides could scavenge free radicals, the DPPH free radical assay is often used. The findings demonstrated the potent DPPH free radical scavenging capacity of the three jujube polysaccharide fractions (Fig. 4A). The activity progressively increased as the concentration rose, indicating a certain concentration dependency. At a concentration of 2.0 mg/mL, the DPPH radical scavenging capacity of the DPZMP3, DZMP, and ZMP were 92.89 %, 89.64 %, and 81.55 %, respectively. Moreover, the IC50 values for three polysaccharide fractions scavenging DPPH radical activity were 0.2174, 0.3153, and 0.4432 mg/mL, respectively. The DPPH scavenging activities of ZP1, ZP2 and ZP3 (extracted using subcritical water and purified using DEAE-52 anion-exchange chromatography) were 74.8 %, 64.9 %, and 88.3 %, respectively, at the concentration of 5.0 mg/mL. The DPPH scavenging activity of DPZMP3 (34.3 kDa) was significantly better than those of ZP1 (874 kDa), ZP2 (765 kDa), and ZP3 (713 kDa), and the differences were particularly significant at the concentration of 2.0 mg/mL (Liu et al., 2020). The findings demonstrated that DPZMP3's capacity to scavenge free radicals was notably greater than that of the other ingredients. Consequently, the comparatively reduced *Mw* of DPZMP3 may be connected to its greater antioxidant action (DPPH free radical). These findings suggested that by breaking down DPZMP3 into a considerably smaller *Mw* fraction, the ultrasound-H_2O_2-Vc therapy might significantly increase the antioxidant activity of DPZMP3 (Wu, He, et al., 2022; Zhao et al., 2006). Degradation of polysaccharides is an effective way to enhance their antioxidant capacity, so having an appropriate molecular weight is an important indicator of good antioxidant activity of polysaccharides.

It is well known that the superoxide anion causes and initiates lipid peroxidation, which further indirectly damages DNA and disrupts regular physiological functions (Li et al., 2022). Superoxide anion radicals are inhibited by plant polysaccharides, and this impact is dose-dependent and ranges from 0.2 to 1.5 mg/mL. At a concentration of 2.0 mg/mL, ZMP, DZMP, and DPZMP3 exhibited superoxide anion radical scavenging activities of 38.48 %, 49.57 %, and 55.96 %, respectively, as seen in Fig. 4B. Comparing DPZMP3 to the others, scavenging activity was significantly greater. DPZMP3 showed higher superoxide radical scavenging activity than LZJP3 (97.66 kDa), extracted from *Zizyphus jujuba cv. Linzexiaozao* and purified successively by DEAE-52 cellulose and Sephadex G-100 column chromatography, at the concentration of 1.0 mg/mL (Li et al., 2011). Because of its high reactivity, the hydroxyl radical may harm a variety of macromolecules, including lipids, amino acids, and nucleic acid. It could also lead to apoptosis and metabolic problems. Consequently, one of the key techniques for assessing plant polysaccharide antioxidant properties *in vitro* is hydroxyl radical scavenging (Liu et al., 2023). The scavenging capacity improved in our research as the content of jujube polysaccharides increased, as seen by Fig. 4C. At concentrations between 0.2 and 1.5 mg/mL, the effects of jujube polysaccharides on oxidative damage caused by hydroxyl radicals were found to be between 3.75 % and 41.82 %; DPZMP3 exhibited the stronger scavenging activity and lower than Vc. Two water-soluble polysaccharides fractions (ZSP1b and ZSP2) were isolated and purified from the fruiting bodies of *Zizyphus Jujuba cv. Jinsixiaozao* by DEAE-SepharoseCL-6B and Sepharose CL-6B column chromatography (Wang et al., 2018). At 2.0 mg/mL, the hydroxyl radical scavenging activity of DPZMP3 (34.3 kDa), ZSP2 (86.0 kDa) and ZSP1b (93.0 kDa) were 41.82 %, 29.9 % and 25.5 %, respectively. Jujube polysaccharide obtained by degradation was more soluble in water due to the breakage of molecular chains, so their active sites could effectively contact with free radicals, thus had better antioxidant activity (Li et al., 2013). The strong antioxidant activity of DPZMP3 is the result of the interaction of several factors, including the rich uronic acid content and low molecular weight. After degradation, lower molecular weight polysaccharides may expose more active groups, and these exposed hydroxyl groups may be the main reason for the increased radical scavenging rate of the polysaccharides obtained by degradation (Li et al., 2020). Overall, the findings indicated that proper ultrasound-assisted H_2O_2-Vc degradation might enhance DPZMP3's antioxidant activity and that the broken-down jujube polysaccharides had promising future uses in the functional food sector.

4. Conclusion

In this work, the effects of ultrasound assisted H_2O_2-Vc system on the physicochemical characteristics and antioxidant activities *in vitro* of a low-molecular-weight jujube polysaccharide from *Ziziphus Jujuba cv. Muzao* were investigated. The reduced *Mw* of DPZMP3 was shown by the results of ultrasound-assisted H_2O_2-Vc reaction. However, there was no discernible alteration in the DPZMP3 functional group or skeleton structure. Furthermore, better results from DPZMP3's *in vitro* antioxidant biological applications were more likely when proper ultrasound-assisted H_2O_2-ascorbic acid therapy was used and DPZMP3 had the potential to be used as a natural polymer antioxidant in food. In order to enhance the bioactivities of jujube polysaccharides in the future, the results point to the possibility of using the ultrasound-H_2O_2/Vc reaction as a degrading technique.

CRediT authorship contribution statement

Yingying Liu: Data curation, Conceptualization. **Yan Meng:** Investigation, Funding acquisition, Conceptualization. **Haozhen Ji:** Resources, Formal analysis, Data curation. **Jianhang Guo:** Validation, Supervision, Software, Conceptualization. **Miaomiao Shi:** Supervision, Investigation, Funding acquisition. **Feiliao Lai:** Writing – review & editing, Validation, Resources. **Xiaolong Ji:** Writing – review & editing, Investigation, Funding acquisition.

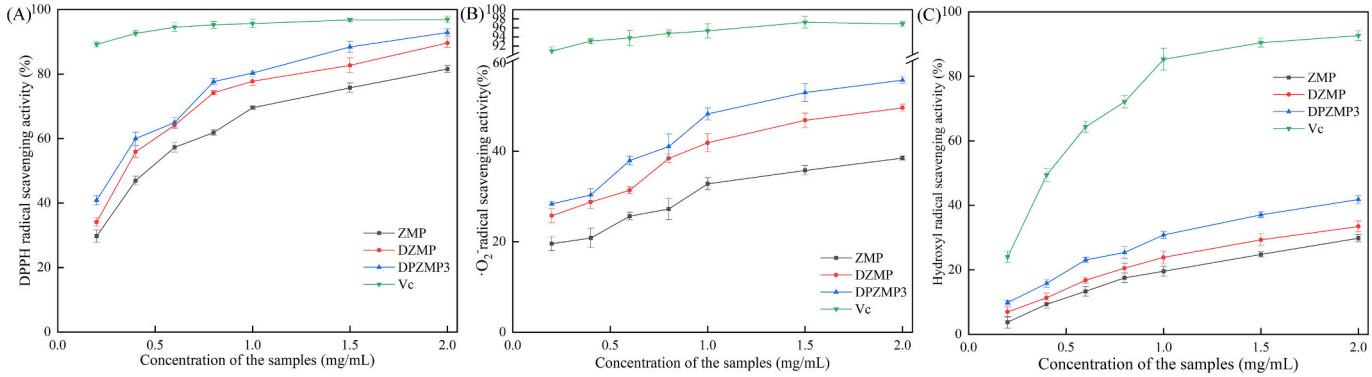

Fig. 4. The antioxidant activities of DPZMP3. (A) DPPH radical scavenging activity. (B) Superoxide radical scavenging activity. (C) OH radical scavenging activity.

Declaration of competing interest

The authors attest that this article does not include any known conflicts of interest.

Data availability

Data will be made available on request.

Acknowledgments

The National Natural Science Foundation of China (No. U21A20297 and 32201969) and Young Scientist Project of Henan Province (No. 225200810122) were used to support this study.

Appendix A. Supplementary data

Supplementary data to this article can be found online at https://doi.org/10.1016/j.fochx.2024.101908.

References

Aafi, E., Ardakani, M. R. S., & Ardakani, M. M. (2022). Jujube (*Ziziphus jujuba* mill. (Rhamnaceae)): A review on its pharmacological properties and phytochemistry. *Traditional Medicine Research, 7*, 66–74. https://doi.org/10.53388/TMR20220905001

Chen, J., Zhang, X., Huo, D., Cao, C., Li, Y., Liang, Y., Li, B., & Li, L. (2019). Preliminary characterization, antioxidant and alpha-glucosidase inhibitory activities of polysaccharides from *Mallotus furetianus*. *Carbohydrate Polymers, 215*, 307–315. https://doi.org/10.3390/molecules27134192

Chen, S., Liu, H., Yang, X., Li, L., Qi, B., Hu, X., Ma, H., Li, C., & Pan, C. (2020). Degradation of sulphated polysaccharides from *Grateloupia livida* and antioxidant activity of the degraded components. *International Journal of Biological Macromolecules, 156*, 660–668. https://doi.org/10.1016/j.ijbiomac.2020.04.108

Fei, Z., Xie, H., Xie, D., Wang, M., Du, Q., & Jin, P. (2024). Structural characterization and high-efficiency prebiotic activity of the polysaccharide from *Tremella aurantialba* endophytic bacteria. *International Journal of Biological Macromolecules, 260*, Article 129347. https://doi.org/10.1016/j.ijbiomac.2024.129347

Gao, Q., Wu, C., & Wang, M. (2013). The jujube (*Ziziphus jujuba* mill.) fruit: A review of current knowledge of fruit composition and health benefits. *Journal of Agricultural and Food Chemistry, 61*, 3351–3363. https://doi.org/10.1021/jf4007032

Guo, J., Xie, J., Yang, X., Yang, S., Liu, Y., & Ji, X. (2024). Degradetion condition optimization and antioxidant activity of jujube polysaccharide. *Food Research and Development, 45*, 99–106. https://doi.org/10.12161/j.issn.1005-6521.2024.01.013

Hajji, M., Hamdi, M., Sellimi, S., Ksouda, G., Laouer, H., Li, S., & Nasri, M. (2019). Structural characterization, antioxidant and antibacterial activities of a novel polysaccharide from *Periploca* laevigata root barks. *Carbohydrate Polymers, 206*, 380–388. https://doi.org/10.1016/j.carbpol.2018.11.020

Hu, B., Zhang, S., Wang, Z., Han, Q., Zhang, D., Zheng, Y., Zheng, K., & Jing, Y. (2023). Degradation method, structural characteristics, biological activity and structure-activity relationship of degraded polysaccharides. *Food Reviews International, 1-30*. https://doi.org/10.1080/87559129.2023.2273933

Ji, X., Cheng, Y., Tian, J., Zhang, S., Jing, Y., & Shi, M. (2021). Structural characterization of polysaccharide from jujube (*Ziziphus jujuba* mill.) fruit. *Chemical and Biological Technologies in Agriculture, 8*. https://doi.org/10.1186/s40538-021-00255-2

Ji, X., Guo, J., Tian, J., Ma, K., & Liu, Y. (2023). Research progress on degradation methods and product properties of plant polysaccharides. *Journal of Light Industry, 38*, 55–62. https://doi.org/10.12187/2023.03.007

Ji, X., Hou, C., Yan, Y., Shi, M., & Liu, Y. (2020). Comparison of structural characterization and antioxidant activity of polysaccharides from jujube (*Ziziphus jujuba* mill.) fruit. *International Journal of Biological Macromolecules, 149*, 1008–1018. https://doi.org/10.1016/j.ijbiomac.2020.02.018

Ji, X., Peng, Q., Li, H., Liu, F., & Wang, M. (2017). Chemical characterization and anti-inflammatory activity of polysaccharides from *Zizyphus jujube cv*. Muzao. *International Journal of Food Engineering, 13*. https://doi.org/10.1515/ijfe-2016-0382

Ji, X., Yan, Y., Hou, C., Shi, M., & Liu, Y. (2020). Structural characterization of a galacturonic acid-rich polysaccharide from *Ziziphus Jujuba cv*. Muzao. *International Journal of Biological Macromolecules, 147*, 844–852. https://doi.org/10.1016/j.ijbiomac.2019.09.244

Ji, X., Zhang, F., Zhang, R., Liu, F., Peng, Q., & Wang, M. (2019). An acidic polysaccharide from *Ziziphus Jujuba cv. Muzao*: Purification and structural characterization. *Food Chemistry, 274*, 494–499. https://doi.org/10.1016/j.foodchem.2018.09.037

Lee, Q., Han, X., Zheng, M., Lv, F., Liu, B., & Zeng, F. (2023). Preparation of low molecular weight polysaccharides from Tremella fuciformis by ultrasonic-assisted H_2O_2-Vc method: Structural characteristics, in vivo antioxidant activity and stress resistance. *Ultrasonics Sonochemistry, 99*, Article 106555. https://doi.org/10.1016/j.ultsonch.2023.106555

Li, B., Liu, S., Xing, R., Li, K., Li, R., Qin, Y., Wang, X., Wei, Z., & Li, P. (2013). Degradation of sulfated polysaccharides from *Enteromorpha prolifera* and their antioxidant activities. *Carbohydrate Polymers, 92*, 1991–1996. https://doi.org/10.1016/j.carbpol.2012.11.088

Li, J., Fan, Y., Huang, G., & Huang, H. (2022). Extraction, structural characteristics and activities of *Zizylphus vulgaris* polysaccharides. *Industrial Crops and Products, 178*, Article 114675. https://doi.org/10.1016/j.indcrop.2022.114675

Li, J., Liu, Y., Fan, L., Ai, L. Z., & Shan, L. (2011). Antioxidant activities of polysaccharides from the fruiting bodies of *Zizyphus Jujuba cv*. Jinsixiaozao. *Carbohydrate Polymers, 84*, 390–394. https://doi.org/10.1016/j.carbpol.2010.11.051

Li, M., Ma, F., Li, R., Ren, G., Yan, D., Zhang, H., Zhu, X., Wu, R., & Wu, J. (2020). Degradation of *Tremella fuciformis* polysaccharide by a combined ultrasound and hydrogen peroxide treatment: Process parameters, structural characteristics, and antioxidant activities. *International Journal of Biological Macromolecules, 160*, 979–990. https://doi.org/10.1016/j.ijbiomac.2020.05.216

Li, X., Zhang, G., Li, J., Jiang, T., Chen, H., Li, P., & Guan, Y. (2021). Degradation by Vc-H_2O_2, characterization and antioxidant activity of polysaccharides from *Passiflora* edulis peel. *Journal of Food Processing and Preservation, 45*, Article e16074. https://doi.org/10.1111/jfpp.16074

Liu, W., Wang, H., Pang, X., Yao, W., & Gao, X. (2010). Characterization and antioxidant activity of two low-molecular-weight polysaccharides purified from the fruiting bodies of *Ganoderma lucidum*. *International Journal of Biological Macromolecules, 46*, 451–457. https://doi.org/10.1016/j.ijbiomac.2010.02.006

Liu, X., Min, L., Yan, Y., Fan, L., Yang, J., Wang, X., & Qin, G. (2020). Structural characterization and antioxidant activity of polysaccharides extracted from jujube using subcritical water. *LWT- Food Science and Technology, 117*, Article 108645. https://doi.org/10.1016/j.lwt.2019.108645

Liu, Y., Guo, Q., Zhang, S., Bao, Y., Chen, M., Gao, L., … Zhou, H. (2023). Polysaccharides from discarded stems of *Trollius chinensis Bunge elicit* promising potential in cosmetic industry: Characterization, moisture retention and antioxidant activity. *Molecules, 28*, 3114. https://doi.org/10.3390/molecules28073114

Lo, T. C., Chang, C. A., Chiu, K. H., Tsay, P. K., & Jen, J. F. (2011). Correlation evaluation of antioxidant properties on the monosaccharide components and glycosyl linkages of polysaccharide with different measuring methods. *Carbohydrate Polymers, 86*, 320–327. https://doi.org/10.1016/j.carbpol.2011.04.056

Ma, G., Yang, W., Mariga, A. M., Fang, Y., Ma, N., Pei, F., & Hu, Q. (2014). Purification, characterization and antitumor activity of polysaccharides from *Pleurotus eryngii* residue. *Carbohydrate Polymers, 114*, 297–305. https://doi.org/10.1016/j.carbpol.2014.07.069

Wang, F., Kong, L., Xie, Y., Wang, C., Wang, X., Wang, Y., Fu, L., & Zhou, T. (2021). Purification, structural characterization, and biological activities of degraded polysaccharides from *Porphyra yezoensis*. *Journal of Food Biochemistry, 45*, Article e13661. https://doi.org/10.1111/jfbc.13661

Wang, Y., Liu, X., Zhang, J., Liu, G., Liu, Y., Wang, K., Yang, M., Cheng, H., & Zhao, Z. (2015). Structural characterization and *in vitro* antitumor activity of polysaccharides from *Zizyphus jujuba cv*. Muzao. *RSC Advances, 5*, 7860–7867. https://doi.org/10.1039/c4ra13350a

Wang, Y., Xu, Y., Ma, X., Liu, X., Yang, M., Fan, W., Ren, H., & Wang, X. (2018). Extraction, purification, characterization and antioxidant activities of polysaccharides from *Zizyphus jujuba cv*. Linzexiaozao. *International Journal of Biological Macromolecules, 118*, 2138–2148. https://doi.org/10.1016/j.ijbiomac.2018.07.059

Wang, Z., Zhou, X., Sheng, L., Zhang, D., Zheng, X., Pan, Y., Yu, X., Liang, X., Wang, Q., Wang, B., & Li, N. (2023). Effect of ultrasonic degradation on the structural feature, physicochemical property and bioactivity of plant and microbial polysaccharides: A review. *International Journal of Biological Macromolecules, 236*, Article 123924. https://doi.org/10.1016/j.ijbiomac.2023.123924

Wu, D., He, Y., Fu, M., Gan, R., Hu, Y., Peng, L., Zhao, G., & Zou, L. (2022). Structural characteristics and biological activities of a pectic-polysaccharide from okra affected by ultrasound assisted metal-free Fenton reaction. *Food Hydrocolloids, 122*, Article 107085. https://doi.org/10.1016/j.foodhyd.2021.107085

Wu, D., Zhao, Y., Yuan, Q., Wang, S., Gan, R., Hu, Y., & Zou, L. (2022). Influence of ultrasound assisted metal-free Fenton reaction on the structural characteristic and immunostimulatory activity of a beta-D-glucan isolated from *Dictyophora indusiata*. *International Journal of Biological Macromolecules, 220*, 97–108. https://doi.org/10.1016/j.ijbiomac.2022.08.058

Yan, S., Pan, C., Yang, X., Chen, S., Qi, B., & Huang, H. (2021). Degradation of *Codium cylindricum* polysaccharides by H_2O_2-Vc-ultrasonic and H_2O_2-Fe^{2+}-ultrasonic treatment: Structural characterization and antioxidant activity. *International Journal of Biological Macromolecules, 182*, 129–135. https://doi.org/10.1016/j.ijbiomac.2021.03.193

Yang, Y., Qiu, Z., Li, L., Vidyarthi, S. K., Zheng, Z., & Zhang, R. (2021). Structural characterization and antioxidant activities of one neutral polysaccharide and three acid polysaccharides from *Ziziphus jujuba cv. Hamidazao*: A comparison. *Carbohydrate Polymers, 261*, Article 117879. https://doi.org/10.1016/j.carbpol.2021.117879

Yeung, Y. K., Kang, Y. R., So, B. R., Jung, S. K., & Chang, Y. H. (2021). Structural, antioxidant, prebiotic and anti-inflammatory properties of pectic oligosaccharides hydrolyzed from okra pectin by Fenton reaction. *Food Hydrocolloids, 118*, Article 106779. https://doi.org/10.1016/j.foodhyd.2021.106779

Yuan, D., Li, C., Huang, Q., & Fu, X. (2020). Ultrasonic degradation effects on the physicochemical, rheological and antioxidant properties of polysaccharide from *Sargassum pallidum*. *Carbohydrate Polymers, 239*, Article 116230. https://doi.org/10.1016/j.carbpol.2020.116230

Zhan, R., Xia, L., Shao, J., Wang, C., & Chen, D. (2018). Polysaccharide isolated fro-m Chinese jujube fruit (*Zizyphus jujuba cv. Junzao*) exerts anti-inflammatory ef-fects

through MAPK signaling. *Journal of Functional Foods, 40*, 461–470. https://doi.org/10.1016/j.jff.2017.11.026

Zhang, Q., Xu, Y., Lv, J., Cheng, M., Wu, Y., Cao, K., Zhang, X., Mou, X., & Fan, Q. (2018). Structure characterization of two functional polysaccharides from *Polygonum multiflorum* and its immunomodulatory. *International Journal of Biological Macromolecules, 113*, 195–204. https://doi.org/10.1016/j.ijbiomac.2018.02.064

Zhao, T., Zhang, Q., Qi, H., Zhang, H., Niu, X., Xu, Z., & Li, Z. (2006). Degradation of porphyran from *Porphyra haitanensis* and the antioxidant activities of the degraded porphyrans with different molecular weight. *International Journal of Biological Macromolecules, 38*, 45–50. https://doi.org/10.1016/j.ijbiomac.2005.12.018

Further-reading

Ji, X., Peng, Q., Yuan, Y., Shen, J., Xie, X., & Wang, M. (2017). Isolation, structures and bioactivities of the polysaccharides from jujube fruit (*Ziziphus jujuba* mill.): A review. *Food Chemistry, 227*, 349–357. https://doi.org/10.1016/j.foodchem.2017.01.074